

Effect of Etch Depth on Strength of Soda-Lime Glass Rods by a Statistical Approach

V. M. Sglavo, R. Dal Maschio & G. D. Sorarù

Dipartimento di Ingegneria dei Materiali, Università degli Studi di Trento, via Mesiano 77, 38050 Trento, Italy

(Received 8 July 1991; revised version received 18 June 1992; accepted 26 June 1992)

Abstract

Hydrofluoric acid solution etching has long been known as a useful method for strengthening glass. In this way surface flaws are at first reduced in length and rounded then completely removed. At this point glass strength depends only on defects emerging from the bulk or on damage produced by the etching reaction products. In this study more than a hundred values of strength of glass rods, etched with hydrofluoric acid, are elaborated by means of a statistical approach, and attention is focused on what have previously been called 'volume defects'. The analysis allows some results about the stress concentration factor of this defects family to be obtained.

Das Ätzen mit Flußsäurelösung ist seit langem als bewährte Methode zur Verstärkung von Glas bekannt. Es wird bewirkt, daß Oberflächendefekte zunächst verkleinert und gerundet und schließlich ganz beseitigt werden. Nun hängt die Festigkeit von Glas nur noch von Defekten aus dem Innern der Probe ab, oder von Fehlern, die durch Reaktionsprodukte der Ätzung erzeugt werden. In dieser Arbeit wurden über hundert Festigkeitswerte von flußsäuregeätzten Glasstäbchen statistisch ausgewertet, wobei der Schwerpunkt auf dem lag, was bisher 'Volumendefekte' genannt wurde. Die Analyse führt zu einigen Ergebnissen über Spannungskonzentrationsfaktoren dieser Defektfamilie.

Il est bien connu que le traitement superficiel à l'acide fluorhydrique en solution est une technique efficace de renforcement des verres. Par cette méthode, les fissures de surface sont, d'abord, réduites en longueur, arrondies et, enfin, complètement éliminées. A ce stade, la résistance mécanique du verre dépend uniquement des défauts présents au coeur du matériau ou des dommages engendrés par la présence des produits de la réaction. Dans cette étude, plus de 100 valeurs de la résistance de baguettes en verre, décapées

à l'acide fluorhydrique, sont traitées par une approche statistique et l'attention est concentrée sur ce que l'on appelle couramment les 'défauts en volume'. L'analyse permet d'obtenir certains résultats concernant le facteur de concentration des contraintes de cette famille de défauts.

1 Introduction

Glass strength is sensitive to surface flaws. A common method of restoring a large portion of pristine strength is by etching glass in hydrofluoric acid solutions.

Proctor¹ proposed two models to explain the strengthening process: the first based on flaw length reduction, the second based on flaw tip rounding. Pavelchek & Doremus² presented a model in which the effect of flaw length reduction was combined with the crack tip rounding. Cooper and co-workers^{3–5} confirmed experimentally the Proctor hypotheses, giving numerical foundation to the theories expressed in the previous papers.

In these papers the fracture strength is connected to the etch depth, according to Proctor's model I, accounting for fracture by bulk flaws. Defining c_B as the half length of the critical bulk flaw and c_{0S} as the initial depth of the critical surface flaw, the fracture strength, $\sigma_{fI}(\delta)$, is given by:

$$\sigma_{fI}(\delta) = \frac{Y_S K_{IC}}{\sqrt{\pi(c_{0S} - \delta)}} \quad (1a)$$

if $(c_{0S} - \delta) > c_B$, or

$$\sigma_{fI}(\delta) = \sigma_{fB} = \frac{Y_B K_{IC}}{\sqrt{\pi c_B}} \quad (1b)$$

if $(c_{0S} - \delta) < c_B$, where K_{IC} is the critical stress intensity factor, δ the etch depth, Y the geometrical flaw shape parameter and the subscripts S and B refer to surface and bulk, respectively.

The experimental results of Ref. 4 are consistent with this model for the early stages of etching, up to a depth of about 50 μm .

Proctor's model II, reviewed in Ref. 4, which attributes strengthening to the increasing of the radius of curvature at the flaw tip, is founded on the relation:

$$\sigma_{\text{fil}}(\delta) = \frac{\sigma_T}{1 + 2\sqrt{\frac{c_0}{\rho_0 + \delta}}} \quad (2)$$

where σ_T is the theoretical strength of the material, $\sigma_{\text{fil}}(\delta)$ is the fracture strength, and ρ_0 the initial crack tip radius, usually ignored with respect to δ .

To accommodate the existence of bulk flaws eqn (2) applies if

$$\frac{\sigma_T}{1 + 2\sqrt{\frac{c_0}{\rho_0 + \delta}}} < \sigma_{\text{cB}}$$

otherwise $\sigma_{\text{fil}}(\delta)$ equals σ_{fB} .

The experimental results of Cooper and coworkers^{3,4} show that starting from an etching depth of about 50 μm , the fracture resistance increases up to etching values of about 200 μm : for greater etching depths, the resistance remains relatively independent of δ . Starting from these experimental evidences Saha & Cooper suggested that perhaps bulk defects are responsible for failure in this etching depth range.

In the present paper a different approach is proposed: experimental fracture strength data for samples etched at different depths and without indentation strength-controlling defects are elaborated by a statistical method. Following this approach, it has been possible to focus on higher strength values, with the goal of investigating what Cooper and coworkers^{3,4} called 'volume defects', characterizing this defects family in respect to the stress concentration factor.

2 Experimental Procedure

Soda-lime glass rods (AR Schott-Ruhrglass GmbH) of 7.0 ± 0.5 mm diameter were cut into 110-mm lengths. They were annealed at 520°C for 24 h to relieve any residual stress. All rods were cleaned in a chromic acid solution and then etched for different times (2–10 min) in a 20 wt% hydrofluoric acid solution at the constant temperature of 35°C. The rods were mounted in a polyethylene holder during etching in a bath kept in agitation by a constant-speed impeller.

After etching, the rods were washed in distilled water and acetone and immediately tested. Every

rod was measured near the ends by a micrometer before and after etching. The samples were immediately broken by four-point bending with an inner and outer span of 20 and 70 mm, respectively, at a constant stressing rate of 100 MPa/s (23°C, 60% RH).

3 Results and Discussion

In order to perform a statistical elaboration of the strength data, the hypothesis has been made that in the etching depth range considered in this work (100–250 μm), the strength distribution was unaffected by different etch depth values.

A surface Weibull distribution function⁶ has been assumed for relating the cumulative probability of failure, P , to the area, A , under tensile stress, σ , so giving:

$$P = 1 - \exp \left[- \int_A \left(\frac{\sigma}{\sigma_0} \right)^m dA \right] \quad (3)$$

where m and σ_0 are the Weibull modulus and a normalizing constant, respectively.

In the present experimental situation, four-point bending of rods, eqn (3) becomes:

$$P = 1 - \exp \left[- KA \left(\frac{\sigma_M}{\sigma_0} \right)^m \right] \quad (4)$$

where

$$K = \frac{1}{\pi} \int_0^\pi (\sin \xi)^m d\xi \quad (4a)$$

$$A = \pi r L \quad (4b)$$

$$\sigma_M = \frac{4Fl}{\pi r^3} \quad (4c)$$

with L the inner span distance, F the applied load, l the distance between internal and external fixture load pins and r the radius of rods.

By ranking statistics, the strengths have been ordered from weakest to strongest with each assigned a probability of failure based on ranking⁷

$$P(\sigma) = \frac{n}{N + 1} \quad (5)$$

where N is the total number of points ($N = 132$). Equation (4) can be rearranged to a straight line by transforming the variables P and σ_M to $\ln \ln(1/(1 - P))$ and $\ln \sigma_M$.

In order to substantiate the starting hypothesis that strength distribution is unaffected by different etch depth values, the strength values have been divided into three groups, each containing about the same number of data. The first group referred to an etch depth between 100 and 160 μm , the second to an

etch depth between 160 and 190 μm and the third to an etch depth between 190 and 250 μm . The data have been elaborated in the manner previously described, taking into account the real diameter of every sample, and plotted in Fig. 1.

The three patterns are well superimposed, confirming the presence of the same families of defects in all the etch depth range considered. After this ascertainment, the experimental data were

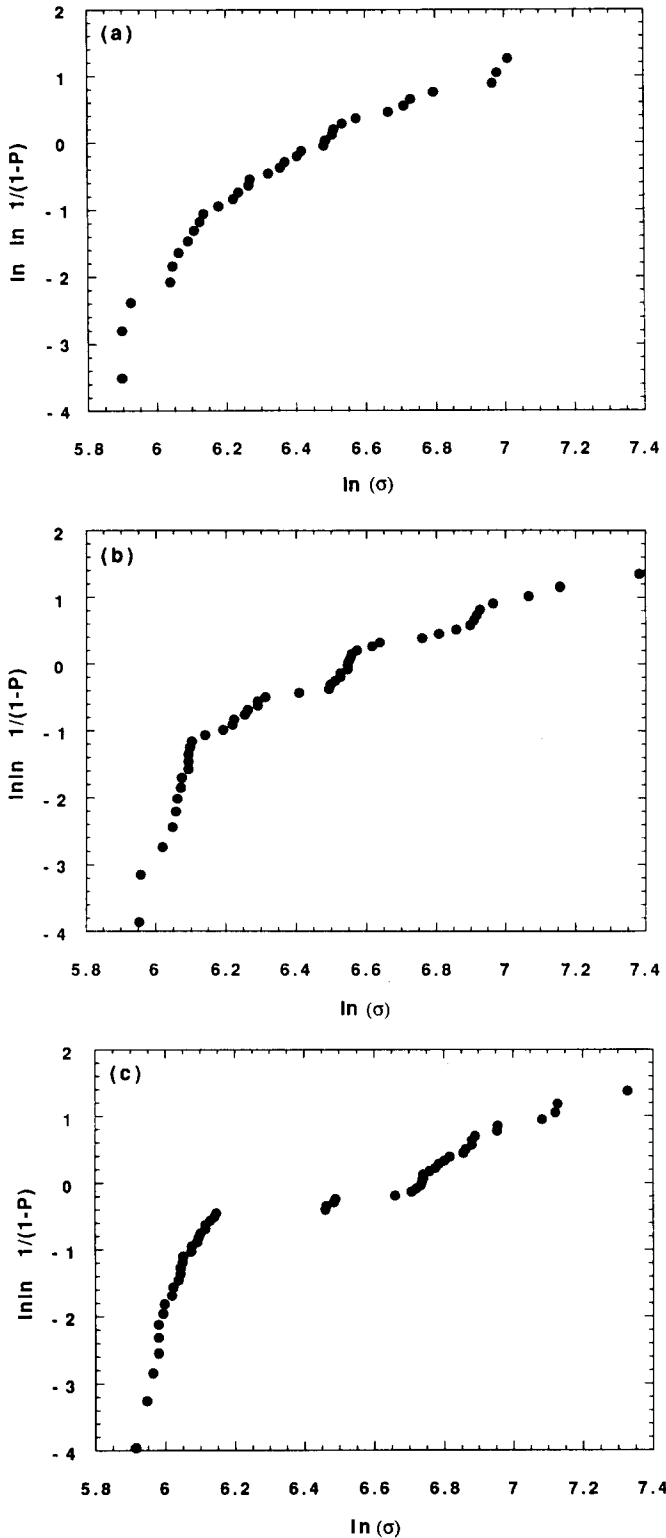


Fig. 1. Weibull plots for experimental resistance data relative to the etch depth ranges: (a) 100–160 μm ; (b) 160–190 μm ; (c) 190–250 μm .

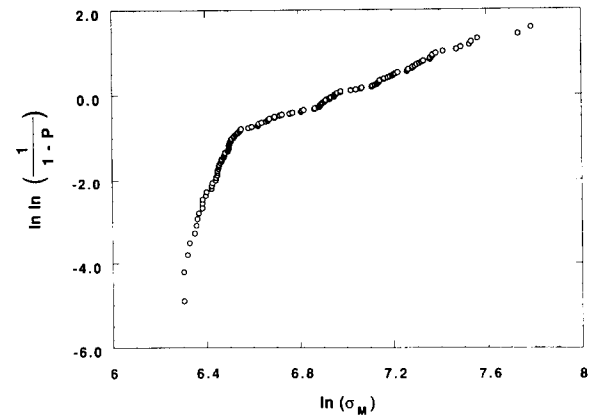


Fig. 2. Weibull plot for the whole experimental resistance data.

elaborated all together and the resultant plot is shown in Fig. 2.

The presence of a bimodal strength distribution is clear. Indeed, it is possible to say that the samples have two distinct fracture origins. It can be said that some specimens fail from defects of type 'A', the others from defects of type 'B'.

According to Johnson,⁷ P_A and P_B are the failure probabilities associated with two surface flaw populations A and B, and P_T the total failure probability function; in the hypothesis that a two-parameter surface Weibull distribution like eqn (5) is valid for both populations, the smallest value of the function

$$\text{sum}(\sigma) = \sum |P_T - P(\sigma)| \quad (6)$$

with the sum extended to all the strength values, has been evaluated by means of the Simplex method applied to non-linear functions.⁸

The hypothesis is made of two partially concurrent surface flaw distributions. So calling A the defect distribution contained in all of the specimens and B the defect distribution present only in a fraction (π_B) of the specimens, the total probability of failure is:

$$P_T = (1 - \pi_B)P_A + \pi_B[1 - (1 - P_A)(1 - P_B)] \quad (7)$$

with P_A and P_B defined as in eqn (5).

The best fit values of π_B , m_A , m_B , σ_{0A} and σ_{0B} have been evaluated in relation to the minimum of the function $\text{sum}(\sigma)$ (Table 1). The corresponding P_T function is represented in Fig. 3, together with the experimental $P(\sigma)$, while P_A and P_B curves are represented in Fig. 4.

It seems reasonable to attribute the broad strength distribution A (with a higher mean strength) to what in other papers are defined as 'bulk

Table 1. Best fit values for the constants of eqn (7)

π_B	σ_{0A}	σ_{0B}	m_A	m_B
0.33	90.24	426.00	3.52	22.49

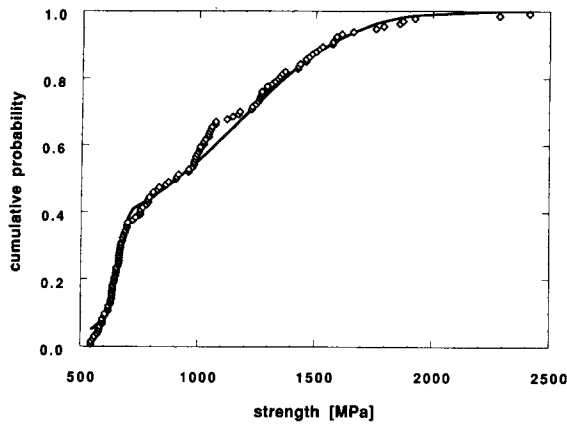


Fig. 3. Plot of fracture cumulative probability: the symbols represent the experimental data, $P(\sigma)$, while the continuous line corresponds to the best fit function, P_T .

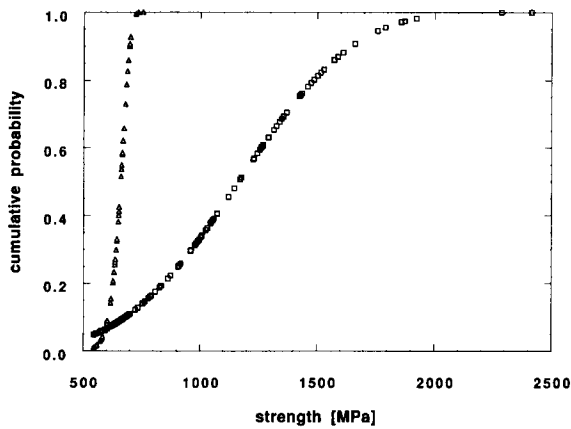


Fig. 4. Plot of calculated (\square) P_A and (\triangle) P_B functions.

flaws^{3,4} and the narrow distribution B to defects created during the etching or manipulation of rods.^{2,5} With this hypothesis, the distribution B can be ignored and attention focused on the high-strength distribution A, which represents the failure probability should defects distribution A be present alone.

Since these experimental strength data are affected by fatigue, as demonstrated well by Roach & Cooper,⁵ the strength in absence of slow crack growth, σ_i , has been evaluated by the following equation:⁹

$$\sigma_i = \left[\frac{BK_{IC}^{n-2}(n-2)\sigma^{n+1}}{2(n+1)\dot{\sigma}} \right]^{1/(n-2)} \quad (8)$$

where B and n are the characteristic data of the crack velocity function:

$$v = \frac{B}{Y^2} K_{IC}^n \quad (9)$$

with Y a geometrical constant, σ the strength in presence of slow crack growth, $\dot{\sigma}$ the stressing rate and K_{IC} the critical stress intensity factor.

B and n values were deduced using the same equation, eqn (9), and the experimental data of Roach & Cooper⁵ with the assumption that defects

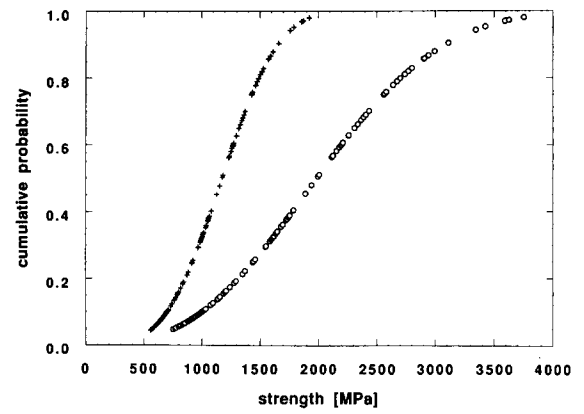


Fig. 5. Plot of (\circ) inert strength distribution; distribution (+) P_A is drawn for comparison.

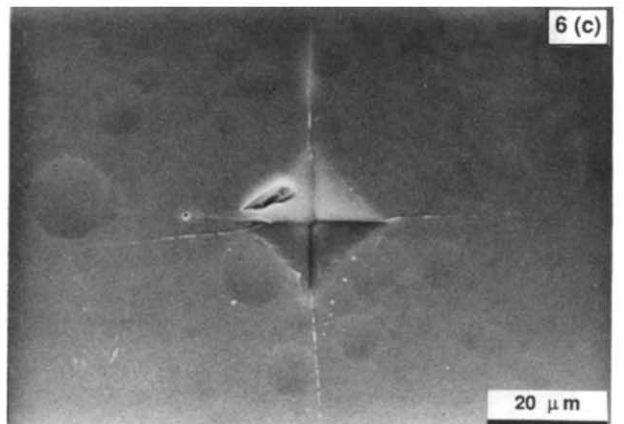
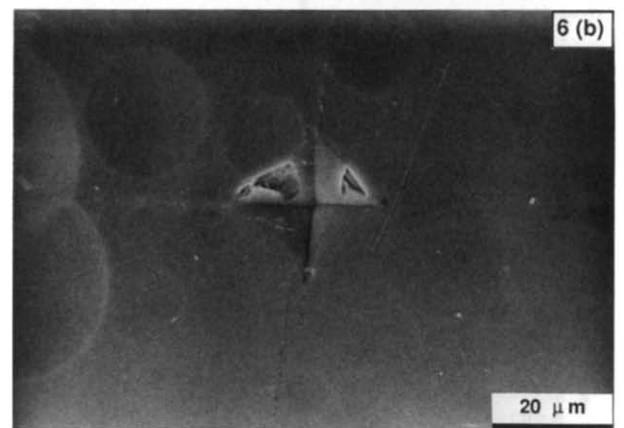
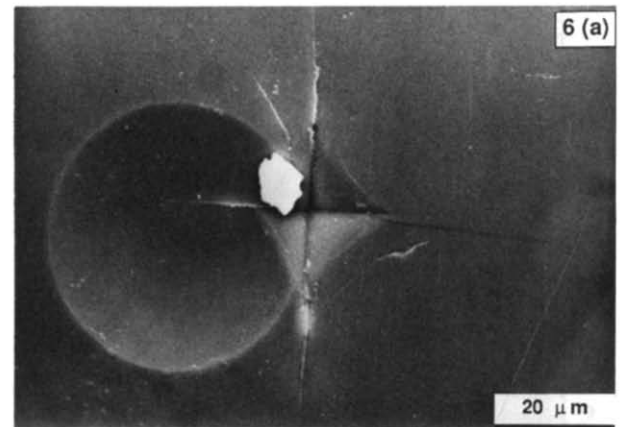


Fig. 6. Hemispherical etch pits on the surface of (a) 130 μm, (b) 190 μm and (c) 250 μm etched rods.

in the samples are geometrically similar (equal Y). The calculated n value (equal to 12.9) is not surprising, as also Dabbs & Lawn¹⁰ found a higher fatigue sensitivity of sub-threshold defects than post-threshold ones.

The inert strength distribution is shown in Fig. 5. It represents the cumulative failure probability of the rods due only to the defect distribution A, in the absence of fatigue.

Figure 6 shows some examples of hemispherical etch pits on the surface of rods for increasing etch depths. The indentations visible on the micrographs have been made after the etching treatment as markers in order to recognize interesting features during SEM analyses. Figure 7 shows very small blisters (0.5–2 μm diameter).

As regards the stress concentration factor, K , which connects the fracture strength, $\sigma(\delta)$, at different etching depths, with the pristine strength of glass, σ_p , according to the equation

$$\sigma(\delta) = \frac{\sigma_p}{K} \quad (10)$$

the formulation proposed by Hara¹¹ relative to spherically surfaced hollows has been considered (Fig. 8). In this situation the stress concentration factor is independent of the dimension of the blister, but rather depending on the ratio h/r connected to

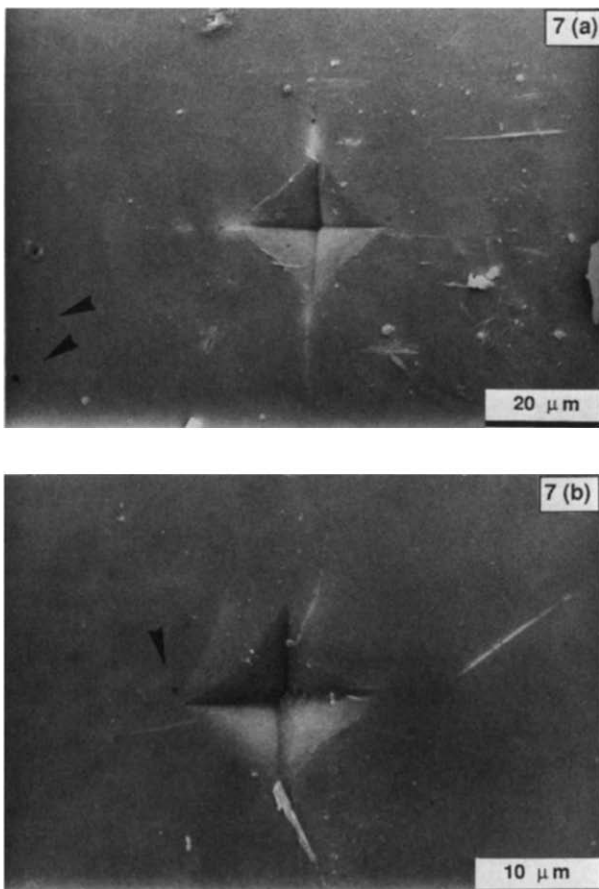


Fig. 7. Blisters (marked by arrows) emerging from the bulk of (a) 130 μm and (b) 240 μm etched rods.

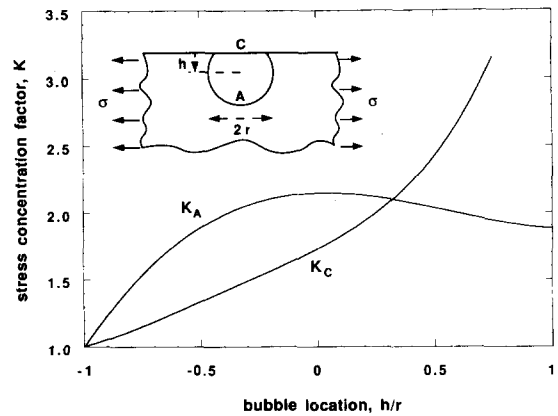


Fig. 8. Stress concentration factor for spherically surfaced hollows as a function of h/r ratio.

bubble location, where h is the distance between the surface and the centre of the bubble and r its radius.

Ishikawa *et al.*¹² demonstrated well that etch pits, derived by HF etching of indentation strength-controlling defects, were the failure loci in bending. In fact the fracture mirrors were observed just beneath the bottom of the etch pits where the maximum stress concentrated.

So, keeping in mind the hemispherical pits in Fig. 6, their ratio h/r is in the range -0.5 to -0.1 , corresponding to a stress concentration factor, K_A , between 1.75 and 2.2. As the intrinsic strength of sheet glass is about 3.4 GPa,¹¹ the fracture strength $\sigma(\delta)$ is in the range 1550–2000 MPa. In the samples where only etch pits with h/r higher than -0.5 (the smallest pits in Fig. 6(c)) the strength increases, but this situation is very fortuitous. As regards blisters in Fig. 7, their ratio h/r is about 0.5, corresponding to a stress concentration factor of about 2.5 and $\sigma(\delta)$ values of about 1300 MPa.

4 Conclusions

A statistical elaboration of experimental strength data of soda-lime glass rods, HF etched, with an etching depth between 100 and 250 μm , has been performed.

The analysis allowed the separation of and focus on one family of defects (etch pits), caused by the etching process, which may be represented and mathematically treated as spherically surfaced hollows. Also, very small blisters, emerging from the bulk owing to the etching process, can be treated in the same manner. The proposed formulation of the stress concentration factor, applied to the different experimental features, allows the large scattering of the strength data to be explained. The inability to eliminate the strength spread seems as intrinsic limit of the process when strength-controlling defects made by indentation are not present.

References

1. Proctor, B., The effects of hydrofluoric acid etching on the strength of glasses. *Phys. Chem. Glasses*, **3**(1) (1962) 7.
2. Pavelchek, E. K. & Doremus, R. H., Fracture strength of soda-lime glass after etching. *J. Mater. Sci.*, **9**(11) (1974) 1803.
3. Roach, D. H. & Cooper, A. R., The effect of etch depth on strength of indented soda lime glass rods. In *Strength of Inorganic Glass*, ed. C. R. Kurkjian. Plenum Press, New York, 1985, pp. 185–95.
4. Saha, C. K. & Cooper, A. R., Effect of etched depth on glass strength. *J. Amer. Ceram. Soc.*, **67**(9) (1984) C158.
5. Roach, D. H. & Cooper, A. R., Weakening of soda-lime glass by particle impact during hydrofluoric acid etching. *J. Amer. Ceram. Soc.*, **69**(8) (1986) C153.
6. Weibull, W., A statistical theory of strength of materials. *Royal Swedish Academy Eng. Sci. Proc.*, **151** (1939) 1.
7. Johnson, C. A., Fracture statistics of multiple flaw distributions. In *Fracture Mechanics of Ceramics*, Vol. 2, ed. R. C. Bradt, D. P. H. Hasselmann & F. F. Lange. Plenum Press, New York, 1974, pp. 365–86.
8. Nelder, J. A. & Mead, R., A Simplex method for function minimization. *Computational J.*, **7** (1965) 308.
9. Wiederhorn, S. M., Evans, A. G., Fuller, E. R. & Johnson, H., Application of fracture mechanics to Space-Shuttle windows. *J. Amer. Ceram. Soc.*, **57**(7) (1974) 319.
10. Dabbs, T. P. & Lawn, B. R., Strength and fatigue properties of optical glass fibers containing microindentation flaws. *J. Amer. Ceram. Soc.*, **68**(11) (1985) 563.
11. Hara, M., Some aspects of strength characteristics of glass. *Glastech. Ber.*, **61** (1988) 7.
12. Ishikawa, H., Shinkai, N. & Sakata, H., Strength of glass with vacuum-deposited metal films: Cr, Al, Au and Ag. *J. Mater. Sci.*, **15** (1980) 483.